Atmos. Chem. Phys. Discuss., 13, 22445–22485, 2013
www.atmos-chem-phys-discuss.net/13/22445/2013/
doi:10.5194/acpd-13-22445-2013

Atmospheric Chemistry and Physics Discussions

A climatology of the diurnal variations of stratospheric and mesospheric ozone over Bern, Switzerland

S. Studer[1,2], **K. Hocke**[1,2], **A. Schanz**[1,2], **H. Schmidt**[3], **and N. Kämpfer**[1,2]

[1]Institute of Applied Physics (IAP), University of Bern, Bern, Switzerland
[2]Oeschger Center for Climate Change Research (OCCR), University of Bern, Bern, Switzerland
[3]Max Planck Institute for Meteorology, Hamburg, Germany

Received: 27 July 2013 – Accepted: 22 August 2013 – Published: 29 August 2013

Correspondence to: S. Studer (simone.studer@iap.unibe.ch)

Published by Copernicus Publications on behalf of the European Geosciences Union.

Abstract

The ground-based radiometer GROMOS, stationed in Bern (47.95° N, 7.44° E), Switzerland, has a unique dataset: it obtains ozone profiles from November 1994 to present with a time resolution of 30 min and equal quality during night- and daytime. Here, we derive a monthly climatology of the daily ozone cycle from 17 yr of GROMOS observation. We present the diurnal ozone variation of the stratosphere and mesosphere. Characterizing the diurnal cycle of stratospheric ozone is important for correct trend estimates of the ozone layer derived from satellite observations. The diurnal ozone cycle from GROMOS is compared to two models: The Whole Atmosphere Community Climate Model (WACCM) and the Hamburg Model of Neutral and Ionized Atmosphere (HAMMONIA). Aura Microwave Limb Sounder (Aura/MLS) ozone data, from night- and daytime overpasses over Bern, have also been included in the comparison. Generally, observation and models show good qualitative agreement: in the lower mesosphere, daytime ozone is for both GROMOS and models around 25 % less than nighttime ozone (reference is 22:30–01:30). In the stratosphere, ozone reaches its maximum in the afternoon showing values several percent larger than the midnight value. It is important that diurnal ozone variations of this order are taken into account when merging different data sets for the derivation of long-term ozone trends in the stratosphere. Further, GROMOS and models indicate a seasonal behavior of daily ozone variations in the stratosphere with a larger afternoon maximum during daytime in summer than in winter. At 0.35 hPa, observations from GROMOS and Aura/MLS show a seasonal pattern in diurnal ozone variations with larger relative amplitudes during daytime in winter (-25 ± 5 %) than in summer (-18 ± 4 %) (compared to mean values around midnight). For the first time, a time series of the diurnal variations in ozone is presented: 17 yr of GROMOS data show strong interannual variations in the diurnal ozone cycle for both the stratosphere and the mesosphere. There are some indications that strong temperature tides can suppress the diurnal variation of stratospheric ozone

ACPD
13, 22445–22485, 2013

via the anticorrelation of temperature and ozone. That means the spatio-temporal variability of solar thermal tides seems to affect the diurnal cycle of stratospheric ozone.

1 Introduction

Studying the diurnal ozone variations can help to test photochemical and transport models (Herman, 1979; Pallister and Tuck, 1983). Additionally, understanding the diurnal variations in ozone is crucial for ozone trend analysis: one difficulty in merging various ozone datasets to create a homogeneous long-term time series is that instruments measure in different sun synchronous orbits and therefore sample data at different local solar times (LST). Combining these different data sets without properly accounting for the diurnal variations of ozone can result in a systematic bias in the determined ozone trend. Further, some satellites drift in orbit over their lifetime. The result being a change of equator-crossing LST and ozone time series which are affected by the diurnal variation of ozone (Bhartia et al., 2012). A comprehensive description of the diurnal ozone variation in the stratosphere is yet missing.

Various papers have discussed the diurnal ozone cycle in the stratosphere and mesosphere. Wilson and Schwartz (1981) used in-situ rocket measurements to study diurnal ozone variations above 48 km. Lobsiger and Künzi (1986) reported on the nighttime increase of mesospheric ozone during winter 1985 and Zommerfelds et al. (1989) assessed the diurnal ozone variations in the mesosphere during winter 1987 using data from ground-based microwave observations for the location of Bern, Switzerland. Ground-based microwave measurements of stratomesospheric ozone from Bordeaux, France were analyzed by Ricaud et al. (1991) and the diurnal cycle of ozone was studied for two layers (at 42 km and 55 km) during three periods in autumn. Using the ozone data set from SABER on the TIMED satellite, Huang et al. (2008, 2010a) derived diurnal ozone variations based on zonal means in the stratosphere and mesosphere.

Model studies on diurnal variations in ozone have been done e.g. by Herman (1979); Pallister and Tuck (1983); Vaughan (1982, 1984); Allen et al. (1984).

ACPD
13, 22445–22485, 2013

Additionally, several comparisons between model and observation were carried out to improve our understanding of the diurnal ozone cycle in the middle atmosphere. Ricaud et al. (1996) used data from the MLS instrument onboard the UARS satellite and compared the results to two photochemical models and with ground-based microwave measurements made from Bordeaux, France. Schneider et al. (2005) showed diurnal ozone variations from the Bordeaux microwave radiometer between 1995 and 2002 and compared their observations to photochemical and transport model results. Haefele et al. (2008) investigated diurnal ozone variations in the stratosphere using ground-based radiometer measurements from Payerne, Switzerland and two chemistry climate models (CCMs). They find that above 2 hPa, ozone strongly decreases during daytime while below 2 hPa, a daytime enhancement in ozone is observed. This behavior is attributed to the $[O]/[O_3]$ ratio which is inversely dependent on air density. Their observed ozone variations in the upper stratosphere and lower mesosphere are in accordance with their used photochemical models. They also note a seasonal dependence of daily ozone variations by looking at March, June and September data (average of 2 yr). Dikty et al. (2010) looked at daytime ozone variations from the HAMMONIA model output and SABER (Sounding of the Atmosphere using Broadband Emission Radiometry) onboard the TIMED (Thermosphere Ionosphere Mesosphere Energetics Dynamics) satellite. Good agreement is found between HAMMONIA and SABER daytime ozone variations in the upper stratosphere. Beig et al. (2012) examined diurnal variations of ozone in the tropics above 1 hPa from HAMMONIA and HALOE onboard UARS. They note that the amplitude of diurnal variation derived from HALOE is slightly lower than that produced by HAMMONIA.

Recently, Sakazaki et al. (2013) presented the global pattern of diurnal ozone variations in the stratosphere from data of the Superconducting Submillimeter-Wave-Emission Sounder (SMILES) attached on the International Space Station (ISS). The observation period was October 2009 to April 2010. They further compared their results to two chemistry-transport models (CTMs). By analyzing CTM data for the underlying mechanisms in the stratospheric diurnal ozone variations, they identified three different

ACPD
13, 22445–22485, 2013

regimes: (1) variations at 20–30 km are caused by dynamics, (2) at 30–40 km, diurnal variations are caused by photochemistry and (3), those at 40–50 km are caused by both dynamics and photochemistry.

The major driver of diurnal variations in the upper stratosphere and lower mesosphere (below 0.01 hPa) is photochemistry (Dikty et al., 2010). Odd oxygen O_x ($O+O_3$) is produced during day through photolysis of molecular oxygen:

$$O_2 + h\nu \rightarrow O + O. \quad (1)$$

Diurnal variations in ozone are dominantly caused by partitioning between O and O_3 in O_x (Sakazaki et al., 2012, 2013). The reactions are described by

$$O + O_2 + M \rightarrow O_3 + M \quad (2)$$

$$O_3 + h\nu \rightarrow O_2 + O \quad (3)$$

where Eq. (2) describes the recombination of molecular and atomic oxygen back to ozone together with a third body M and Eq. (3) represents the photolysis of ozone by solar radiation. Photochemical box models can reproduce and explain the daytime depletion in the upper stratosphere and the afternoon maximum in the middle stratosphere. When diurnal ozone variations of observations are compared to models, they are generally well reproduced in the upper stratosphere and mesosphere.

In contrast, no clear picture exists for diurnal variations of ozone in the middle and lower stratosphere. Not only photochemistry, but dynamics (e.g. through the vertical transport by diurnal tides) contribute to the daily ozone variations. Compared to the mesosphere, amplitudes in the stratosphere are much smaller and in the order of a few percent. The diurnal cycle in stratospheric ozone is therefore difficult to measure and not a lot of adequate observations exist. Model simulations on the other hand may have difficulty in correctly implementing dynamical features, such as e.g. a possible diurnal

ACPD
13, 22445–22485, 2013

cycle in the gravity wave flux and vertical winds. The high spatio-temporal variability of atmospheric tides in the middle atmosphere e.g. can only be described by specialized simulations of advanced models and is a challenging research topic of middle atmospheric dynamics (Ortland and Alexander, 2006).

Diurnal ozone variations can be further affected through the dependence of chemical reaction rates on temperature tides. An early study by Barnett et al. (1975) showed that there is an anticorrelation between ozone and temperature variations near the stratopause. Finger et al. (1995), using SBUV ozone and NCEP/CPC temperature data, find that while in the upper stratosphere and lower mesosphere ozone and temperature are generally negatively correlated, in the lower stratosphere the correlation between them is positive. This is due to the dependence of photochemical reaction rates on temperature. Recently, Huang et al. (2012) analyzed the ozone-temperature diurnal correlation using TIMED/SABER data from 2004 to 2007. They show varying patterns of diurnal variations, depending on altitude and latitude and note that both ozone and temperature diurnal variations show systematic and regular phase progression in LST. Additionally, other reactions such as ClO_x-, HO_x- and NO_x-chemistry can affect the diurnal ozone cycle in both mesosphere and stratosphere (Pallister and Tuck, 1983; Brasseur and Solomon, 2005; Khosravi et al., 2012). Pallister and Tuck (1983) noted the importance of active nitrogen chemistry at 40 km while active hydrogen dominates above 43 km.

The millimeter-wave radiometer GROMOS, stationed in Switzerland, continuously retrieves ozone profiles since November 1994. GROMOS is part of the Network for the Detection of Atmospheric Composition Change (NDACC). It obtains ozone profile in the stratosphere and lower mesosphere with equal quality during day- and nighttime. With a time series of nearly 20 yr and a time resolution of 30 min, GROMOS is ideally suited to study the diurnal ozone variations at midlatitudes.

In this study we analyze diurnal variations in ozone from 17 yr of GROMOS observation. The manuscript is organized as follows. In Sect. 2, data sets from GROMOS and models are described, while Sect. 3 describes the methods of data analysis. Section 4

ACPD
13, 22445–22485, 2013

presents a monthly mean climatology of diurnal ozone variations from 50 to 0.2 hPa (~ 21 to 59 km). We further compare results from GROMOS with the model outcomes from WACCM and HAMMONIA. Section 5 focuses on the mean seasonal variations (January to December) of the diurnal ozone cycle at 5.7 hPa (~ 35 km) and at 0.35 hPa (~ 55 km). In Sect. 6, the interannual variability of the daily cycle on these two pressure levels is investigated. Conclusions are given in Sect. 7. Previous studies of diurnal ozone variatons have mainly been based on limited time periods. Here, using 17 yr of GROMOS observation, we show for the first time a full seasonal climatology as well as interannual variations of the diurnal ozone cycle for a midlatitude station.

2 Data sources

2.1 GROMOS radiometer

Since November 1994, the millimeter-wave radiometer GROMOS (GROund-based Millimeter-wave Ozone Spectrometer) is operated continuously at Bern, Switzerland (47.95° N, 7.44° E). GROMOS observes the middle atmosphere in north-east direction through detection of the collision broadened emission of the ozone transition at 142.17504 GHz. GROMOS is part of the Network for the Detection of Atmospheric Composition Change (NDACC) and its data set is used for cross-validation of satellite experiments, studies of ozone-climate interactions and middle atmospheric dynamics, as well as for long-term monitoring of the ozone layer in the stratosphere (Peter and Kämpfer, 1995; Peter et al., 1996; Calisesi et al., 2001; Dumitru et al., 2006; Hocke et al., 2006; Steinbrecht et al., 2006; Hocke et al., 2007; Flury et al., 2009; Steinbrecht et al., 2009; Studer et al., 2012; Hocke et al., 2013).

From November 1994 to October 2011, a filter bench has been used for spectral analysis. In July 2009, GROMOS has been upgraded and a Fast-Fourier-Transfom spectrometer (FFTS) is used additionally as backend. The data set used here is the ozone time series from the 17 yr of filter bench measurements.

ACPD
13, 22445–22485, 2013

The 45-channel filter bench had a bandwidth of 1.2 GHz with a frequency resolution varying from 200 kHz at the line center to 100 MHz at the wings. Since the middle atmospheric signal is attenuated by the troposphere (mainly due to water vapor), a tropospheric correction is applied to the observed spectra. A spin-off from the tropospheric correction is the estimation of the tropospheric opacity τ (for more information see Lobsiger et al., 1984; Lobsiger, 1987; Ingold et al., 1998).

From the tropospheric corrected line spectrum, ozone volume mixing ratio (VMR) profiles are determined in the retrieval process. The retrieval of GROMOS ozone profiles is based upon the optimal estimation method of Rodgers (Rodgers, 1976) as implemented by the Arts/Qpack software (Eriksson et al., 2005, 2011). Bandwidth and frequency resolution allow the retrieval of ozone profiles from approximately 25 to 65 km. With an integration time of 30 min, the total relative error of retrieved VMR profiles is in the order of 7 % for the stratosphere and increases toward the lower and upper altitude limit (up to 20 % at 20 km and up to 30 % at 70 km). The GROMOS radiometer is described in more detail by Peter (1997).

2.2 WACCM model

The Whole Atmosphere Community Climate Model (WACCM) is a community access model which was developed by the National Center of Atmospheric Research (NCAR) in Boulder, Colorado (Garcia et al., 2007; Marsh et al., 2007; Tilmes et al., 2007). The model consists of individual land, ice, ocean and atmospheric model components. They interact within the software framework of the Community Earth System Model (CESM) where a coupler merges and brokers the data exchange. For our numerical simulation we used version 4 of WACCM with a pre-configured simulation scenario called F 2000. This configuration reads climatologies of sea surface temperatures and ice coverage. The stub land model part satisfies the coupler needs. Atmosphere and land model are simulated actively within this configuration. The WACCM chemistry module is from the Model for OZone And Related chemical Tracers, version 3 (MOZART-3), which includes detailed stratospheric chemistry (Kinnison et al., 2007). WACCM is capable

ACPD
13, 22445–22485, 2013

of reproducing the tidal seasonality. Using WACCM simulations, Pedatella et al. (2012) investigated solar tide changes in the mesosphere and above that occur in response to sudden stratospheric warmings. In order to simulate short term ozone variations, the model time step was downscaled to 15 min. For the comparison here, the grid point for Bern is 46° N and 5° E and the output is saved every 4 model steps, resulting in a time resolution of 1 h. The vertical resolution of WACCM ranges from 1.1 km in the lower stratosphere to 3.5 above 65 km.

2.3 HAMMONIA model

HAMMONIA (Hamburg Model of the Neutral and Ionized Atmosphere) is a three-dimensional general circulation and chemistry model developed at the Max Planck Institute for Meteorology in Hamburg, Germany (Schmidt et al., 2006). It is based on the ECHAM 5 atmospheric general circulation model (Roeckner et al., 2003, 2006). HAMMONIA includes important atmospheric dynamics, radiation, and chemistry and treats them interactively. It covers an approximate altitude range from the surface to 250 km on 119 pressure layers. HAMMONIA, like WACCM, is coupled to the MOZART chemistry module (MOZART-3). Dikty et al. (2010) compared upper mesospheric daytime variations (6 a.m. to 6 p.m.) of ozone and temperature in the tropics from HAMMONIA and SABER observation. In a more recent paper by Beig et al. (2012), diurnal ozone and temperature variations of the equatorial mesosphere are studied by using HALOE satellite data and the HAMMONIA model on the 24 h time scale. Analysis of the diurnal (Achatz et al., 2008) and semidiurnal (Yuan et al., 2008) thermal tides in the mesosphere and lower thermosphere in HAMMONIA data show that many important aspects of tidal observations are reproduced by the model.

The model output from HAMMONIA used in this manuscript are 3-hourly ozone values and the closest grid point to Bern at 45° N and 7.5° E has been taken for the comparison with GROMOS. We therefore have 8 ozone model values per day for the location of Bern. The vertical resolution increases from about 700 m in the lower and middle stratosphere to about 3 km in the middle mesosphere.

ACPD
13, 22445–22485, 2013

3 Data analysis

3.1 Ozone spectra from GROMOS

For our analysis we averaged monthly LST sorted data from 17 yr of GROMOS to obtain mean emission lines of ozone at 142 GHz (depending on LST). This prevents us from studying day to day variations but allows us to derive a monthly climatology. Time bins are chosen as 0 a.m./ 1 a.m./ 2 a.m./ ... / 23 a.m. UT ±1 h, giving us 24 spectra per month. The overlapping time intervals allow us to have a longer integration time and have the advantage that single too low or too high values don't affect the rest of the sample as much.

Figure 1 shows the 24 mean intensity spectra of April 2008 (different colors). Per time interval, the averaged number of individual tropospheric corrected spectra to obtain the mean spectrum vary, depending on the month and the time. The number of spectra averaged for one month ranges from around 800 to 1200. Spectra measured during times (summer months) of high atmospheric opacity (tropospheric opacity larger than 1.2) are not included. Integration over one month is done to reduce the noise on the data. The standard deviation is approx. 3 K at the line center and 1 K at the line wing, while the error of mean ranges from 0.1 K (line center) to 0.03 K (line wing).

Figure 1a and b show the full spectra calculated by using the median (a) and the arithmetic mean values (b), respectively. A zoom of the line center is given in Fig. 1c and d. Figure 1d shows larger fluctuations than c. The median calculation is generally more robust and is able to suppress the influence from individual bad data which sometimes can pass the outlier rejection routines. Bad data can exist due to fluctuations of single filter bench channels and time periods of high opacity values.

Figure 1c also shows nicely the increase of ozone at nighttime (thick blue line), where the peak at the line center is strongest due to the increase of mesospheric ozone.

ACPD
13, 22445–22485, 2013

3.2 Ozone profiles from GROMOS

The retrieved profile is a mix of an a priori guess and information from the measurement. For GROMOS, the a priori ozone profiles are taken as a monthly mean climatology where no diurnal variation is included.

Figure 2 (left panel) shows the mean retrieved profiles for January at Bern during nighttime (blue line) and daytime (magenta line), together with the a priori profile for January (red). The nighttime ozone increase in the mesosphere, as well as a daytime increase around 35 km is apparent. The two middle panels of Fig. 2 give the GROMOS averaging kernel (AVK) matrix for nighttime, respectively daytime. AVKs for altitude levels of 28 (blue), 40 (purple) and 52 (red) km are enhanced and they peak at the corresponding altitude. The vertical resolution can be estimated by the full width at half maximum (FWHM) and lies within 10 to 20 km. The right panel of Fig. 2 shows the mean a priori contribution in percent for night- and daytime observations (blue, respectively magenta). The a priori contributions are nearly identical and GROMOS measures with equal night- and daytime quality.

The generally low vertical resolution of ground-based microwave radiometers should be taken into account in comparison studies with other (higher resolution) instruments and models. This is usually done by convolving the high resolution data with the AVKs of the low resolution instrument. Here, we decided not to smooth model data with our GROMOS AVKs since the aim is to characterize the diurnal variations and not to impose the limited resolution of radiometer measurements to models, in which case interesting features might get lost.

For the analysis therefore, no degrading of the vertical resolution of the models has been done. The model data has been interpolated onto the same vertical pressure grid. All data presented are ozone volume mixing ratios (VMRs).

ACPD
13, 22445–22485, 2013

3.3 Derivation of daily ozone cycle

The diurnal variations of ozone at the location of Bern for GROMOS and models were calculated by

$$\Delta O_{3,abs} = O_3 - O_{3,nmean} \quad (4)$$

$$\Delta O_{3,rel} = \frac{O_3 - O_{3,nmean}}{O_{3,nmean}} \quad (5)$$

where the mean nighttime ozone values $O_{3,nmean}$ is taken by monthly averaging the time interval 11:30 p.m. to 1:30 a.m. at each pressure level. For the climatology of diurnal ozone variations of GROMOS, the error of the mean values including the natural variability is estimated by the standard deviation σ_i from 17 yr of measurements, where the index $i = 1:24$ gives the hourly time bin i based on LST. Model simulations from WACCM and HAMMONIA included one model year (representative for all years of observation). Interannual variation of the diurnal ozone cycle is studied only by using GROMOS data.

4 Diurnal cycle of ozone

4.1 GROMOS

Figure 3a, 3b, 3c, 3d give the mean diurnal ozone variations from 17 yr of GROMOS measurements. Representative for winter, spring, summer and autumn, January, April, July and October are shown. Plotted are LST variations in ozone and diurnal variations $\Delta O_{3,abs}$ (Eq. 4) in absolute as well as $\Delta O_{3,rel}$ (Eq. 5) in relative units from 50 to 0.2 hPa. Magenta lines indicate a solar zenith angle (SZA) of 90° which roughly corresponds to sunrise and sunset.

ACPD
13, 22445–22485, 2013

The rapid repartitioning between O and O_3 can be seen clearly by the sharp transition at sunrise and sunset between high nighttime and low daytime ozone abundances in the mesosphere. Generally, the amplitude of the diurnal variation increases with decreasing pressure. This is due to the slower recombination of O_3 (Eq. 2) relative to the rate of O_3 photolysis (Eq. 3) (Allen et al., 1984). The mean diurnal variation for April (Fig. 3b) is in agreement with Zommerfelds et al. (1989), who also see a daytime decrease in the ozone contectration of −30 % (compared to nighttime ozone) for April 1987 at 56 km over Bern.

Moving down in altitude into the stratosphere, we find a transition: Daytime ozone depletion switches to a daytime increase in ozone by a few percent. Around 5 hPa, an afternoon maximum of approximately 4 % in winter and 6 % in summer can be seen around 3 p.m.).

Note, that ozone volume mixing ratios are larger in the summer stratosphere compared to winter (6.5 ppm versus 7.5 ppm).

4.2 Comparison between GROMOS and models

Figure 4a and 4b are equal to Fig. 3c but show the unconvolved outputs from WACCM, respectively HAMMONIA. The month of July has been chosen for the comparison since the stratosphere in summer is less disturbed compared to winter when planetary wave activity is high. Further, a smaller year-to-year variation is found in summer measurements than for winter where dynamical processes are strong (planetary waves). It is important to note that, as mentioned in Sects. 2.2 and 2.3, both models use the chemistry mechanism MOZART. Other components of the models such as dynamical cores and physical parameterization are different.

Models and GROMOS agree generally well. Both show a similar pattern of diurnal variations with similar amplitudes. Some differences are pointed out: (1) The altitude level at which data show a change from strong ozone destruction to an ozone increase during daytime is not the same. While GROMOS sees this around 2 hPa, both models show the transition around stratopause level (1 hPa). This difference in transition alti-

ACPD
13, 22445–22485, 2013

tude between observation and model has also been noted by (Scheiben et al., 2013), who studied the diurnal variations of middle atmospheric water vapor. (2) The afternoon maximum appears at a slightly higher altitude in the models than for GROMOS observations (around 3 hPa). (3) WACCM and HAMMONIA, both, show a phase progression in local time as a function of altitude, which is not seen by GROMOS.

Some of the discrepancies may be related to the limited altitude resolution of GROMOS. It has to be noted, that the altitude difference between 2 hPa and 3 hPa is only 3 km and possibly cannot be resolved by GROMOS.

The downward phase progression in the model results of WACCM and HAMMONIA (Fig. 4a and 4b) from around 1 hPa in the morning (around 6 a.m.) to approximately 3 hPa in the afternoon (around 4 p.m.) has been noted before in thermal tides: Huang et al. (2010b) derived diurnal temperature variations (migrating tides) from SABER on TIMED. They note that transport by tides can affect ozone diurnal variations in a similar way (Huang et al., 2010a). It has to be kept in mind that, GROMOS, measuring at a fixed location, cannot separate migrating and non-migrating tides. At the end of the day, there is a another shift of the ozone maximum towards higher altitudes. This has been discussed for the mesosphere by Marsh et al. (2003) and attributed to the temperature dependent production rate of HO_x. GROMOS cannot confirm these modeling results.

Figures 5a and 5b show the diurnal ozone variations for mean January and July on four pressure levels (approx. at 55, 45, 35 and 25 km). GROMOS is given in blue (together with standard deviation σ_i) and the models are given in black (WACCM) and red (HAMMONIA). Additionally, the relative difference between nighttime and daytime overpasses for Bern (1:30 a.m./p.m. LST) from the MLS instrument onboard the Aura satellite are given as green diamonds. January and July data from Aura/MLS data were average for the time period 2004 to 2011.

At 55 km, the daytime amplitudes from models in January are slightly smaller than for GROMOS and Aura/MLS sees an even smaller variation. For July, the amplitude of all data sets (except for Aura/MLS) are found to be in very good agreement (−25 %). A reason for the off-value from Aura/MLS might be, that the satellite data are not con-

ACPD
13, 22445–22485, 2013

volved with GROMOS AVKs. Please note that no significant nighttime variation is seen in all data sets.

At 1.42 hPa, GROMOS measures a decrease in ozone during daytime (−5 to −7 %), while models already switched to a slight increase. Observation by the Mauna Loa microwave instrument (Parrish et al., 2012) for March (average of 1996–2012) shows also a decrease of −5 % at 1.3 hPa, supporting our measurements. The phase nevertheless is slightly shifted: GROMOS measures the minimum at about 12 p.m., while Parrish et al. (2012) give 1 to 2 p.m.

For 5.8 hPa in January, an afternoon maximum (of approx. 3 %) is found at 3 p.m., agreeing very well with the observation from Aura/MLS. The WACCM and HAMMONIA do not show a diurnal variation (amplitude < 1 %). The Mauna Loa microwave instrument measures also an amplitude of approx. +3 %, again for March. The phase is again shifted by about 2 h (3 p.m. for the radiometer at Mauna Loa and 1 p.m. for GROMOS in Bern). For July, the diurnal amplitude of GROMOS increases up to +6 % around 4 pm. The models also show a daily variation with an afternoon maximum at 4 pm of +3 %. While for January models mostly are within the GROMOS σ-bars, they do not overlap for July.

For 25 km, σ-values are larger than the diurnal ozone amplitudes which do not exceed 1 % for all data sets. Hence, if there is a diurnal cycle in the lower stratosphere, amplitudes are very small (at midlatitudes). It is not possible to draw any further conclusions.

5 Seasonal variation of the diurnal ozone cycle

We looked at the mean seasonal variation for two fixed pressure levels. Figure 6 shows the diurnal cycle as a function of month (January to December) in the stratosphere at 5.76 hPa. The results from GROMOS (a) are compared to the WACCM output (b). Magenta lines indicate again sunrise and sunset. The behavior of HAMMONIA is very similar (not shown here).

ACPD
13, 22445–22485, 2013

The afternoon maximum is clearly visible in both, observation and model for all month. They further agree on stronger diurnal afternoon amplitudes in summer than for winter. They do vary though on the amplitude strength. GROMOS peaks in July with +6 % and WACCM peaks from May to August with +3 %. When looking at a slightly higher level (3.3 hPa) in WACCM data (not shown here), the agreement is much better and WACCM also shows a seasonal maximum of +5 % in July.

WACCM shows a decrease of ozone by about −1 % after sunrise in all seasons except winter, an effect not measured by GROMOS. This dawn minimum has already been seen in the model results by Pallister and Tuck (1983). They attributed this depletion of ozone in the morning to the chemistry of NO_x.

Figure 7 is as Fig. 6, but for the mesosphere at 0.35 hPa. The general seasonal variation agrees and daytime depletion of ozone is around −25 %. An intriguing feature is that while GROMOS shows a stronger day to night variation in winter (up to −30 % in November), WACCM has the largest diurnal amplitude in summer (with a relative amplitude of −26 %). Figure 8 shows the time series of relative night-to-day ratios from Aura/MLS at 0.38 hPa (black line). A moving average of the time series can be found by the red line of Fig. 8. An annual cycle with larger relative night-to-day ratios in winter than for summer is supporting the GROMOS observations from Fig. 7. Further studies on the seasonal dependency of the diurnal ozone cycle are needed to help understand and resolve this discrepancy between the WACCM model and measurements.

6 Interannual variation of the diurnal ozone cycle

We used the 17 yr of GROMOS measurement to study the interannual variation of diurnal variations in ozone. Figure 9 presents the results for the two pressure levels 5.76 hPa and 0.35 hPa from Sect. 5. As in Figs. 6 and 7, we find the diurnal amplitude to be larger in summer than winter at 5.76 hPa and smaller in summer than winter at 0.35 hPa. Nevertheless, 9 shows that there are strong interannual variations in both

ACPD
13, 22445–22485, 2013

stratosphere and mesosphere. Averaging several years of data therefore might not capture the diurnal behavior of specific years.

We tried to verify the strong decrease of GROMOS daytime ozone in winter 2006 in the mesosphere (at 0.35 hPa) by looking again at the Aura/MLS data of Fig. 8. Aura/MLS also shows a stronger than usual ozone decrease during daytime for February 2006, but the values of the previous and next month do not show as large amplitudes. The large negative values during daytime in winter 2006 might be linked to the strong sudden stratospheric warming (SSW) event, described by Manney et al. (2009). However, other SSWs seem not to have such a prominent signal.

The anomaly at sunrise in the stratosphere of summer 2000 might be explained by an anomaly of NO_x in the stratosphere (Gebhardt et al., 2013). Another possible reason for the anomaly in summer 2000 is the temperature dependence of ozone. As mentioned in the introduction, ozone and temperature perturbations are anticorrelated in the upper stratosphere. This is illustrated in Fig. 10. It shows the day-night differences of stratospheric ozone and temperature (moving average over 12 months) using data from ECMWF (European Centre for Medium-Range Weather Forecast) (2.5 to 5.5 hPa). The correlation coefficient is $R = -0.75$ (± 0.07) at the 95 % confidence level. In summer 2000, the anomaly of Fig. 10 (low ΔO_3, large ΔT) supports the low daytime anomaly seen in GROMOS data of Fig. 9a. The signal in temperature and ozone (small ΔT and large ΔO_3) of 1998 in Fig. 10 might be related to the enhanced El Niño Southern Oscillation (ENSO) activity of that year and a stronger excitation of thermal tides. Pedatella and Liu (2012) investigated the migrating and non-migrating variability of tides in the mesosphere and lower thermosphere due to the ENSO based on WACCM simulations. Recently, they also found that the ENSO-driven variability in the migrating diurnal tide is found to be primarily due to changes in the tropospheric forcing (Pedatella and Liu, 2013). We suppose that the increase of temperature during daytime leads to a reduced accumulation of ozone during daytime (temperature-dependence of ozone photochemistry).

ACPD
13, 22445–22485, 2013

7 Conclusions

Stratospheric and mesospheric ozone, measured by the radiometer GROMOS from 17 yr of observation, has been analyzed in order to study its diurnal variability from 50 to 0.2 hPa (~ 21–59 km). A climatology of the diurnal ozone cycle above Bern, Switzerland, is presented. The observational results from GROMOS have been compared with simulation outputs from the WACCM and the HAMMONIA model. Additionally, the two local solar times of overpasses over Bern from Aura/MLS have been included in the intercomparison.

We find that observation and models are generally consistent. Amplitudes in the mesosphere are in the order of −25 % and in the stratosphere an afternoon maximum in the order of +4 % is apparent. The sharp phase transition from nighttime ozone enhancement at mesospheric altitudes to daytime ozone enhancement in the middle and upper stratosphere occurs in the model simulations approximately 3 km higher than in the GROMOS measurements.

We investigated for the first time the seasonal variability of the diurnal cycle. The long-term climatology derived from the GROMOS measurements at Bern shows:

1. a larger relative diurnal amplitude during summer months for the stratosphere. For the pressure level of 5.8 hPa, the amplitude is +6 % in summer, while for winter the amplitude is in the order of +3 %,

2. a smaller relative diurnal amplitude during summer compared to winter in the mesosphere. At 0.35 hPa, the diurnal amplitude in winter is up to −30 %, while for summer it is around −22 %.

Opposed to the latter result, mesospheric WACCM outputs show a larger mesospheric amplitude during summer compared to winter.

Further, by looking at the time series of the diurnal ozone cycle from 17 yr of GROMOS time series, we find a strong interannual variability. Indications are found that

ACPD
13, 22445–22485, 2013

temperature tides influence the diurnal variation of stratospheric ozone which is due to the temperature-dependent ozone photochemistry.

Our observational results indicate that the seasonal and interannual variability of the diurnal variation of stratospheric ozone have to be considered when correcting satellite data for the diurnal ozone signal to estimate stratospheric ozone trends. Therefore, ongoing effort is needed in order to improve our knowledge of the diurnal ozone variations in the stratosphere. For this reasons, a team of scientists from various observation and model communities have built up a team at the International Space Science Institute (ISSI) with the goal to tackle the still unresolved subject on "Characterizing Diurnal Variations of Ozone".

Acknowledgements. This research was funded by the Swiss National Science Foundation SNF under grant no. 200020-134613. The research leading to these results has received funding from the European Community's Seventh Framework Programme ([FP7/2007-2013]) under grant agreement no. 284421 (see Article II.30. of the Grant Agreement). We thank the MLS-team for the ozone data used in this study which was retrieved from the NASA Goddard Space Flight Center. This work was further supported by the International Space Science Institute (ISSI) in Bern, Switzerland. We would like to thank members of the first workshop held at ISSI on the subject "Characterizing Diurnal Variations of Ozone for Improving Ozone Trend Estimates" for discussions and inputs (http://www.issibern.ch/teams/ozonetrend/).

References

Achatz, U., Grieger, N., and Schmidt, H.: Mechanisms controlling the diurnal solar tide: Analysis using a GCM and a linear model, J. Geophys. Res.: Space Physics, 113, A08303, doi:10.1029/2007JA012967, 2008. 22453

Allen, M., Lunine, J. I., and Yung, Y. L.: The vertical distribution of ozone in the mesosphere and lower thermosphere, J. Geophys. Res.-Atmos., 89, 4841–4872, doi:10.1029/JD089iD03p04841, 1984. 22447, 22457

Barnett, J. J., Houghton, J. T., and Pyle, J. A.: The temperature dependence of the ozone concentration near the stratopause, Q. J. Roy. Meteorol. Soc., 101, 245–257, doi:10.1002/qj.49710142808, 1975. 22450

ACPD
13, 22445–22485, 2013

Beig, G., Fadnavis, S., Schmidt, H., and Brasseur, G. P.: Inter-comparison of 11-year solar cycle response in mesospheric ozone and temperature obtained by HALOE satellite data and HAMMONIA model, J. Geophys. Res.-Atmos., 117, D00P10, doi:10.1029/2011JD015697, 2012. 22448, 22453

Bhartia, P. K., McPeters, R. D., Flynn, L. E., Taylor, S., Kramrova, N. A., Frith, S., Fisher, B., and DeLand, M.: Solar Backscatter UV (SBUV) total ozone and profile algorithm, Atmos. Meas. Tech. Discuss., 5, 5913–5951, doi:10.5194/amtd-5-5913-2012, 2012. 22447

Brasseur, G. P. and Solomon, S.: Aeronomy of the Middle Atmosphere: Chemistry and Physics of the Stratosphere and Mesosphere, Springer, 2005. 22450

Calisesi, Y., Werli, H., and Kaempfer, N.: Midstratospheric ozone variability over Bern related to planetary wave activity during the winters 1994–1995 to 1998–1999, J. Geophys. Res., 106, 7903–7916, 2001. 22451

Dikty, S., Schmidt, H., Weber, M., von Savigny, C., and Mlynczak, M. G.: Daytime ozone and temperature variations in the mesosphere: a comparison between SABER observations and HAMMONIA model, Atmos. Chem. Phys., 10, 8331–8339, doi:10.5194/acp-10-8331-2010, 2010. 22448, 22449, 22453

Dumitru, M. C., Hocke, K., Kaempfer, N., and Calisesi, Y.: Comparison and validation studies related to ground-based microwave observations of ozone in the stratosphere and mesosphere, J. Atmos. Sol.-Terr. Phys., 68, 745–756, 2006. 22451

Eriksson, P., Jiménez, C., and Buehler, S. A.: Qpack, a general tool for instrument simulation and retrieval work, J. Quant. Spectrosc. Ra., 91, 47–64, doi:10.1016/j.jqsrt.2004.05.050, 2005. 22452

Eriksson, P., Buehler, S. A., Davis, C. P., Emde, C., and Lemke, O.: ARTS, the atmospheric radiative transfer simulator, Version 2, J. Quant. Spectrosc. Ra., 112, 1551–1558, doi:10.1016/j.jqsrt.2011.03.001, 2011. 22452

Finger, F. G., Nagatani, R. M., Gelman, M. E., Long, C. S., and Miller, A. J.: Consistency between variations of ozone and temperature in the stratosphere, Geophys. Res. Lett., 22, 3477–3480, doi:10.1029/95GL02786, 1995. 22450

Flury, T., Hocke, K., Haefele, A., Kämpfer, N., and Lehmann, R.: Ozone depletion, water vapor increase, and PSC generation at midlatitudes by the 2008 major stratospheric warming, J. Geophys. Res., 114, D18302, doi:10.1029/2009JD011940, 2009. 22451

ACPD
13, 22445–22485, 2013

Garcia, R. R., Marsh, D. R., Kinnison, D. E., Boville, B. A., and Sassi, F.: Simulation of secular trends in the middle atmosphere, 1950–2003, J. Geophys. Res.-Atmos., 112, D09301, doi:10.1029/2006JD007485, 2007. 22452

Gebhardt, C., Rozanov, A., Hommel, R., Weber, M., Bovensmann, H., Burrows, J. P., Degenstein, D., Froidevaux, L., and Thompson, A. M.: Stratospheric ozone trends and variability as seen by SCIAMACHY during the last decade, Atmos. Chem. Phys. Discuss., 13, 11269–11313, doi:10.5194/acpd-13-11269-2013, 2013. 22461

Haefele, A., Hocke, K., Kämpfer, N., Keckhut, P., Marchand, M., Bekki, S., Morel, B., Egorova, T., and Rozanov, E.: Diurnal changes in middle atmospheric H_2O and O_3: Observations in the Alpine region and climate models, J. Geophys. Res.-Atmos., 113, D17303, doi:10.1029/2008JD009892, 2008. 22448

Herman, J. R.: The response of stratospheric constituents to a solar eclipse, sunrise, and sunset, J. Geophys. Res.-Oceans, 84, 3701–3710, doi:10.1029/JC084iC07p03701, 1979. 22447

Hocke, K., Kämpfer, N., Feist, D. G., Calisesi, Y., Jiang, J. H., and Chabrillat, S.: Temporal variance of lower mesospheric ozone over Switzerland during winter 2000/2001, Geophys. Res. Lett., 33, L09801, doi:10.1029/2005GL025496, 2006. 22451

Hocke, K., Kämpfer, N., Ruffieux, D., Froidevaux, L., Parrish, A., Boyd, I., von Clarmann, T., Steck, T., Timofeyev, Y. M., Polyakov, A. V., and Kyrölä, E.: Comparison and synergy of stratospheric ozone measurements by satellite limb sounders and the ground-based microwave radiometer SOMORA, Atmos. Chem. Phys., 7, 4117–4131, doi:10.5194/acp-7-4117-2007, 2007. 22451

Hocke, K., Studer, S., Martius, O., Scheiben, D., and Kämpfer, N.: A 20-day period standing oscillation in the northern winter stratosphere, Ann. Geophys., 31, 755–764, doi:10.5194/angeo-31-755-2013, 2013. 22451

Huang, F. T., Mayr, H. G., Russell, J. M., Mlynczak, M. G., and Reber, C. A.: Ozone diurnal variations and mean profiles in the mesosphere, lower thermosphere, and stratosphere, based on measurements from SABER on TIMED, J. Geophys. Res.-Space Physics, 113, A04307, doi:10.1029/2007JA012739, 2008. 22447

Huang, F. T., Mayr, H. G., Russell, J. M., and Mlynczak, M. G.: Ozone diurnal variations in the stratosphere and lower mesosphere, based on measurements from SABER on TIMED, J. Geophys. Res.-Atmos., 115, D24308, doi:10.1029/2010JD014484, 2010a. 22447, 22458

Huang, F. T., McPeters, R. D., Bhartia, P. K., Mayr, H. G., Frith, S. M., Russell, J. M., and Mlynczak, M. G.: Temperature diurnal variations (migrating tides) in the stratosphere and

ACPD
13, 22445–22485, 2013

lower mesosphere based on measurements from SABER on TIMED, J. Geophys. Res.-Atmos., 115, D16121, doi:10.1029/2009JD013698, 2010b. 22458

Huang, F. T., Mayr, H. G., Russell, J. M., and Mlynczak, M. G.: Ozone-Temperature Diurnal and Longer Term Correlations, in the Lower Thermosphere, Mesosphere and Stratosphere, Based on Measurements from SABER on TIMED, Tech. Rep. GSFC.JA.00222.2012, NASA Technical Report, Goddard Space Flight Center; Langley Research Center, http://naca.larc.nasa.gov/, 2012. 22450

Ingold, T., Peter, R., and Kämpfer, N.: Weighted mean tropospheric temperature and transmittance determination at milimeter-wave frequencies for ground-based application, Radio Sci., 33, 905–918, 1998. 22452

Khosravi, M., Baron, P., Urban, J., Froidevaux, L., Jonsson, A. I., Kasai, Y., Kuribayashi, K., Mitsuda, C., Murtagh, D. P., Sagawa, H., Santee, M. L., Sato, T. O., Shiotani, M., Suzuki, M., von Clarmann, T., Walker, K. A., and Wang, S.: Diurnal variation of stratospheric and lower mesospheric HOCl, ClO and HO_2 at the equator: comparison of 1-D model calculations with measurements by satellite instruments, Atmos. Chem. Phys., 13, 7587–7606, doi:10.5194/acp-13-7587-2013, 2013. 22450

Kinnison, D. E., Brasseur, G. P., Walters, S., Garcia, R. R., Marsh, D. R., Sassi, F., Harvey, V. L., Randall, C. E., Emmons, L., Lamarque, J. F., Hess, P., Orlando, J. J., Tie, X. X., Randel, W., Pan, L. L., Gettelman, A., Granier, C., Diehl, T., Niemeier, U., and Simmons, A. J.: Sensitivity of chemical tracers to meteorological parameters in the MOZART-3 chemical transport model, J. Geophys. Res.-Atmos., 112, D20302, doi:10.1029/2006JD007879, 2007. 22452

Lobsiger, E.: Ground-based microwave radiometry to determine stratospheric and mesospheric ozone profiles, J. Atmos. Terr. Phys., 49, 493–501, 1987. 22452

Lobsiger, E. and Künzi, K. F.: Night-time increase of mesospheric ozone mea269 sured with ground-based microwave radiometry, J. Atmos. Terr. Phys., 48, 1153–1158, 1986. 22447

Lobsiger, E., Künzi, K. F., and Dütsch, H. U.: Comparison of stratospheric ozone profiles retrieved from microwave-radiometer and Dobson-spectrometer data, J. Atmos. Terr. Phys., 46, 799–806, 1984. 22452

Manney, G. L., Harwood, R. S., MacKenzie, I. A., Minschwaner, K., Allen, D. R., Santee, M. L., Walker, K. A., Hegglin, M. I., Lambert, A., Pumphrey, H. C., Bernath, P. F., Boone, C. D., Schwartz, M. J., Livesey, N. J., Daffer, W. H., and Fuller, R. A.: Satellite observations and modeling of transport in the upper troposphere through the lower mesosphere dur-

ACPD
13, 22445–22485, 2013

ing the 2006 major stratospheric sudden warming, Atmos. Chem. Phys., 9, 4775–4795, doi:10.5194/acp-9-4775-2009, 2009. 22461

Marsh, D., Smith, A., and Noble, E.: Mesospheric ozone response to changes in water vapor, J. Geophys. Res.-Atmos., 108, 4109, doi:10.1029/2002JD002705, 2003. 22458

Marsh, D. R., Garcia, R. R., Kinnison, D. E., Boville, B. A., Sassi, F., Solomon, S. C., and Matthes, K.: Modeling the whole atmosphere response to solar cycle changes in radiative and geomagnetic forcing, J. Geophys. Res.-Atmos., 112, D23306, doi:10.1029/2006JD008306, 2007. 22452

Ortland, D. A. and Alexander, M. J.: Gravity wave influence on the global structure of the diurnal tide in the mesosphere and lower thermosphere, J. Geophys. Res.Space Physics, 111, A10S10, doi:10.1029/2005JA011467, 2006. 22450

Pallister, R. C. and Tuck, A. F.: The diurnal variation of ozone in the upper stratosphere as a test of photochemical theory, Q. J. Roy. Meteorol. Soc., 109, 271–284, doi:10.1002/qj.49710946002, 1983. 22447, 22450, 22460

Parrish, A., Boyd, I., Nedoluha, G., Bhartia, P. K., Frith, S., Connor, B., Bodeker, G., and Froidevaux, L.: Diurnal Variations of Stratospheric Ozone Measured by Ground-based Microwave Remote Sensing at the Mauna Loa NDACC site: Measurement Validation and Results, in: Quadrannial Ozone Symposium, Toronto, 2012. 22459

Pedatella, N. M. and Liu, H.-L.: Tidal variability in the mesosphere and lower thermosphere due to the El Niño Southern Oscillation, Geophys. Res. Lett., 39, L19802, doi:10.1029/2012GL053383, 2012. 22461

Pedatella, N. M. and Liu, H.-L.: Influence of the El Niño Southern Oscillation on the middle and upper atmosphere, J. Geophys. Res.-Space Physics, 118, 2744–2755, doi:10.1002/jgra.50286, 2013. 22461

Pedatella, N. M., Liu, H.-L., Richmond, A. D., Maute, A. I., and Fang, T.-W.: Simulations of solar and lunar tidal variability in the mesosphere and lower thermosphere during sudden stratosphere warmings and their influence on the low-latitude ionosphere, J. Geophys. Res., 117, A08326, doi:10.1029/2012JA017858, 2012. 22453

Peter, R.: The ground-based millimeter-wave ozone spectrometer-GROMOS, IAP Research Report, University of Bern, Switzerland, 13, 1997. 22452

Peter, R. and Kämpfer, N.: Short-term variations of mid-latitude ozone profiles during the winter 1994/95, Proc. Third Europ. Symp. on Polar O3 Res., 484–487, 1995. 22451

ACPD
13, 22445–22485, 2013

Peter, R., Calisesi, Y., and Kämpfer, N.: Variability of middle atmospheric ozone abundances derived from continuous ground-based millimeter wave measurements, Atmospheric Ozone, Bojkov, R. D. and Visconti, G., Vol. 2, Proceedings of the XVIII Quadrennial Ozone Symposium, International Ozone Commission, 559–562, 1996. 22451

Ricaud, P., Brillet, J., De La Noe, J., and Parisot, J. P.: Diurnal and seasonal variations of stratomesospheric ozone: Analysis of ground-based microwave measurements in Bordeaux, France, J. Geophys. Res.-Atmos., 96, 18617–18629, doi:10.1029/91JD01871, 1991. 22447

Ricaud, P., de La No, J., Connor, B. J., Froidevaux, L., Waters, J. W., Harwood, R. S., MacKenzie, I. A., and Peckham, G. E.: Diurnal variability of mesospheric ozone as measured by the UARS microwave limb sounder instrument: Theoretical and ground-based validations, J. Geophys. Res.-Atmos., 101, 10077–10089, doi:10.1029/95JD02841, 1996. 22448

Rodgers, C. D.: Retrieval of atmospheric temperature and composition from remote measurements of thermal radiation, Rev. Geophys., 14, 609–624, doi:10.1029/RG014i004p00609, 1976. 22452

Roeckner, E., G. Bäuml, G., Bonaventura, L., Brokopf, R., Esch, M., Giorgetta, M., Hagemann, S., Kirchner, I., Kornblueh, L., Manzini, E., Rhodin, A., Schlese, U., Schulzweida, U., and Tompkins, A.: The atmospheric general circulation model ECHAM 5. PART I: Model description, MPI Tech. Report 349, Max Planck Institute for Meteorology, Hamburg, Germany, 2003. 22453

Roeckner, E., Brokopf, R., Esch, M., Giorgetta, M., Hagemann, S., Kornblueh, L., Manzini, E., Schlese, U., and Schulzweida, U.: Sensitivity of Simulated Climate to Horizontal and Vertical Resolution in the ECHAM5 Atmosphere Model, J. Climate, 19, 4841–4872, doi:10.1175/JCLI3824.1, 2006. 22453

Sakazaki, T., Fujiwara, M., Mitsuda, C., Imai, K., Manago, N., Naito, Y., Nakamura, T., Akiyoshi, H., Kinnison, D., T., S., Suzuki, M., and Shiotani, M.: Diurnal Ozone Variations in the Stratosphere as Revealed with SMILES Observations, in: Quadrannial Ozone Symposium, Toronto, 2012. 22449

Sakazaki, T., Fujiwara, M., Mitsuda, C., Imai, K., Manago, N., Naito, Y., Nakamura, T., Akiyoshi, H., Kinnison, D., Sano, T., Suzuki, M., and Shiotani, M.: Diurnal ozone variations in the stratosphere revealed in observations from the Superconducting Submillimeter-Wave Limb-Emission Sounder (SMILES) on board the International Space Station (ISS), J. Geophys. Res.-Atmos., 118, 2991–3006, doi:10.1002/jgrd.50220, 2013. 22448, 22449

ACPD
13, 22445–22485, 2013

Scheiben, D., Schanz, A., Tschanz, B., and Kämpfer, N.: Diurnal variations in middle-atmospheric water vapor by ground-based microwave radiometry, Atmos. Chem. Phys., 13, 6877–6886, doi:10.5194/acp-13-6877-2013, 2013. 22458

Schmidt, H., Brasseur, G. P., Charron, M., Manzini, E., Giorgetta, M. A., Diehl, T., Fomichev, V. I., Kinnison, D., Marsh, D., and Walters, S.: The HAMMONIA chemistry climate model: Sensitivity of the mesopause region to the 11-year solar cycle and CO_2 Doubling, J. Climate, 19, 3903–3931, doi:10.1175/JCLI3829.1, 2006. 22453

Schneider, N., Selsis, F., Urban, J., Lezeaux, O., Noe, J., and Ricaud, P.: Seasonal and Diurnal Ozone Variations: Observations and Modeling, J. Atmos. Chem., 50, 25–47, doi:10.1007/s10874-005-1172-z, 2005. 22448

Steinbrecht, W., Claude, H., Schönenborn, F., McDermid, I., Leblanc, T., Godin, S., Song, T., Swart, D., Meijer, Y., Bodeker, G., Connor, B., Kämpfer, N., Hocke, K., Calisesi, Y., Schneider, N., Noe, J., Parrish, A., Boyd, I., Brühl, C., Steil, B., Giorgetta, M., Manzini, E., Thomasson, L., Zawodny, J., McCormick, M., Russel III, J., Bhartia, P., Stolarski, R., and Hollandsworth-Frith, S.: Long-Term Evolution of Upper Stratospheric Ozone at Selected Stations of the Network for the Detection of Stratospheric Change (NDSC), J. Geophys. Res., 111, D10308, doi:10.1029/2005JD006454, 2006. 22451

Steinbrecht, W., Claude, H., Schönenborn, F., McDermid, I., LeBlanc, T., Godin-Beekmann, S., Keckhut, P., Hauchecorne, A., van Gijsel, J., Swart, D., Bodeker, G., Parrish, A., Boyd, I., Kämpfer, N., Hocke, K., Stolarski, R., Frith, S., Thomason, L., Remsberg, E., von Savigny, C., Rozanov, A., and Burrows, J.: Ozone and temperature trends in the upper stratosphere at five stations of the Network for the Detection of Atmospheric Composition Change, Int. J. Remote Sens., 30, 3875–3886, 2009. 22451

Studer, S., Hocke, K., and Kämpfer, N.: Intraseasonal oscillations of stratospheric ozone above Switzerland, J. Atmos. Sol.-Terr. Phys., 74, 189–198, doi:10.1016/j.jastp.2011.10.020, 2012. 22451

Tilmes, S., Kinnison, D. E., Garcia, R. R., Müller, R., Sassi, F., Marsh, D. R., and Boville, B. A.: Evaluation of heterogeneous processes in the polar lower stratosphere in the Whole Atmosphere Community Climate Model, J. Geophys. Res.-Atmos., 112, D24301, doi:10.1029/2006JD008334, 2007. 22452

Vaughan, G.: Diurnal variation of mesospheric ozone, Nature, 296, 133–135, doi:10.1038/296133a0, 1982. 22447

ACPD
13, 22445–22485, 2013

Vaughan, G.: Mesospheric ozone theory and observation, Q. J. Roy. Meteorol. Soc., 110, 239–260, doi:10.1002/qj.49711046316, 1984. 22447

Wilson, W. J. and Schwartz, P. R.: Diurnal variations of mesospheric ozone using millimeter-wave measurements, J. Geophys. Res.-Oceans, 86, 7385–7388, doi:10.1029/JC086iC08p07385, 1981. 22447

Yuan, T., Schmidt, H., She, C. Y., Krueger, D. A., and Reising, S.: Seasonal variations of semidiurnal tidal perturbations in mesopause region temperature and zonal and meridional winds above Fort Collins, Colorado (40.6° N, 105.1° W), J. Geophys. Res., 113, D20103, doi:10.1029/2007JD009687, 2008. 22453

Zommerfelds, W. C., Kunzi, K. F., Summers, M. E., Bevilacqua, R. M., Strobel, D. F., Allen, M., and Sawchuck, W. J.: Diurnal variations of mesospheric ozone obtained by ground-based microwave radiometry, J. Geophys. Res.-Atmos., 94, 12819–12832, doi:10.1029/JD094iD10p12819, 1989. 22447, 22457

ACPD
13, 22445–22485, 2013

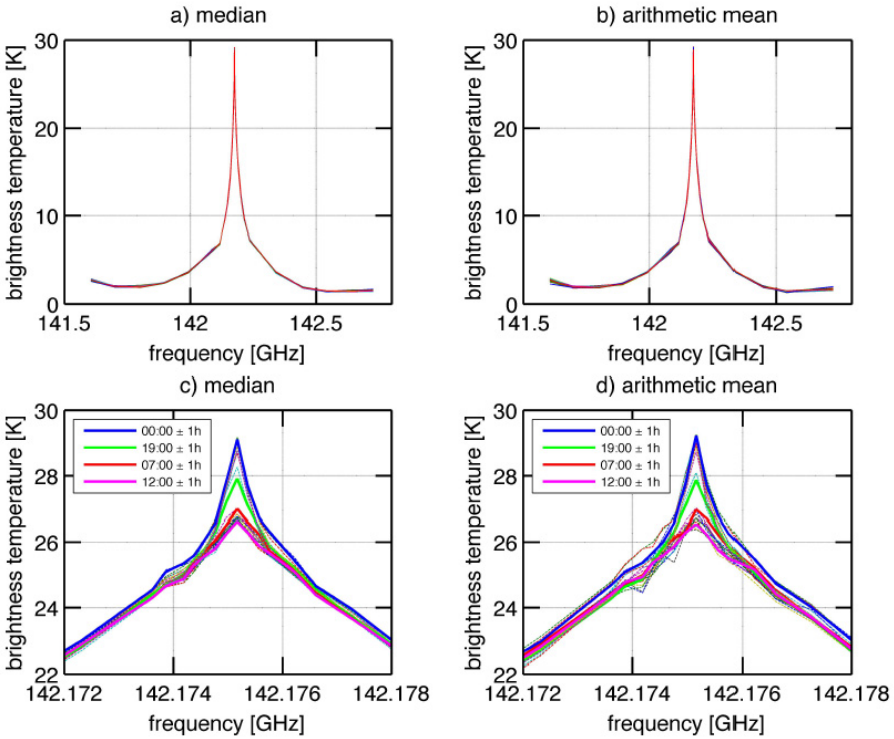

Fig. 1. GROMOS spectra for April 2008, averaged with **(a)** median and **(b)** arithmetic mean. The averaged time intervals are taken as 00:00, 01:00, 02:00, ... 23:00 UT ±1 h, from all days of April 2008, resulting in 24 spectra per month. Different colors correspond to different time bins. A zoom into the line center is given in **(c)** for the median calculation and **(d)** for the arithmetic mean, respectively. Four time bins are highlighted by the thick lines.

ACPD
13, 22445–22485, 2013

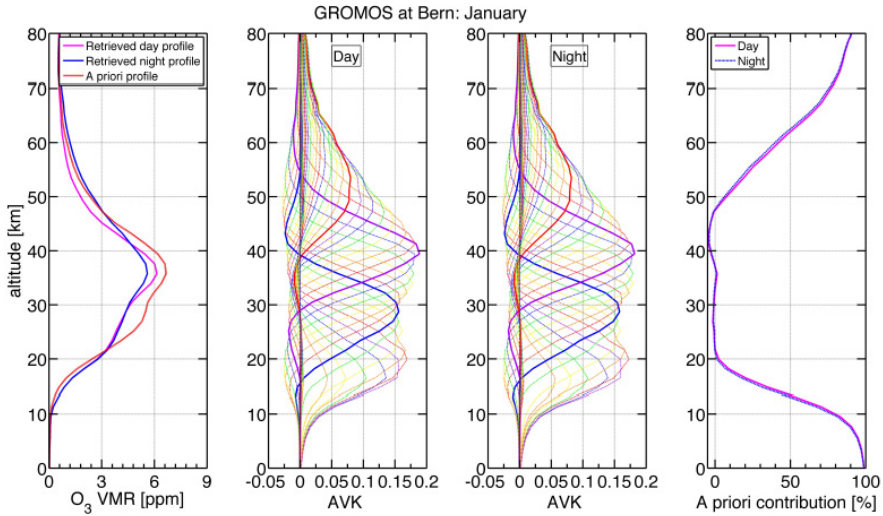

Fig. 2. Averaged GROMOS daytime (magenta) and nighttime (blue) profiles for January 2010 as well as the apriori profile (red) are given in the left panel. In the two middle panels, one finds the daytime and respectively nighttime averaging kernel (AVK) matrix for January. The a priori contribution to the retrieved daytime (magenta) and nighttime (blue) profiles is shown in the right panel.

ACPD
13, 22445–22485, 2013

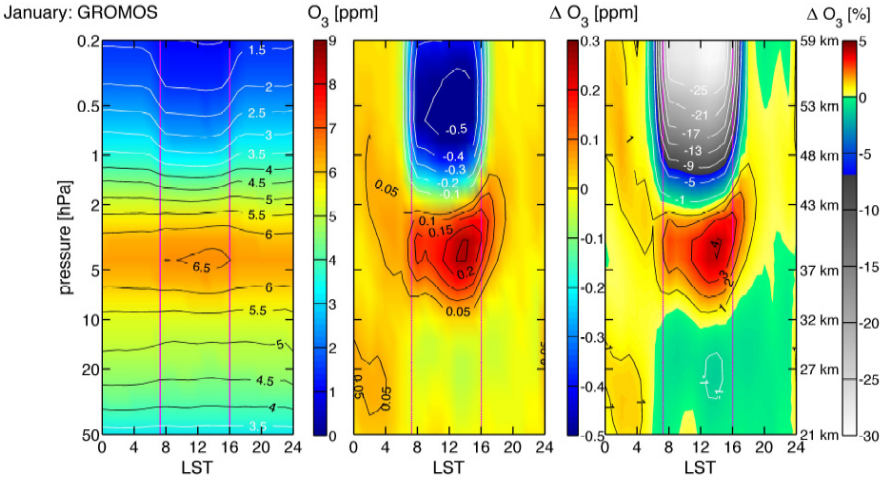

Fig. 3a. Mean diurnal ozone variation of GROMOS between 50 and 0.2 hPa for January. The left panel shows the variation of ozone volume mixing ratios (VMR) as a function of local solar time (LST). The center panel gives the absolute mean difference, while the right panel shows the relative mean difference ΔO_3 in percent. Both, absolute and relative mean differences, are with respect to the mean nighttime value (22:30–01:30) of January. Magenta lines indicate a solar zenith angle of 90°.

ACPD
13, 22445–22485, 2013

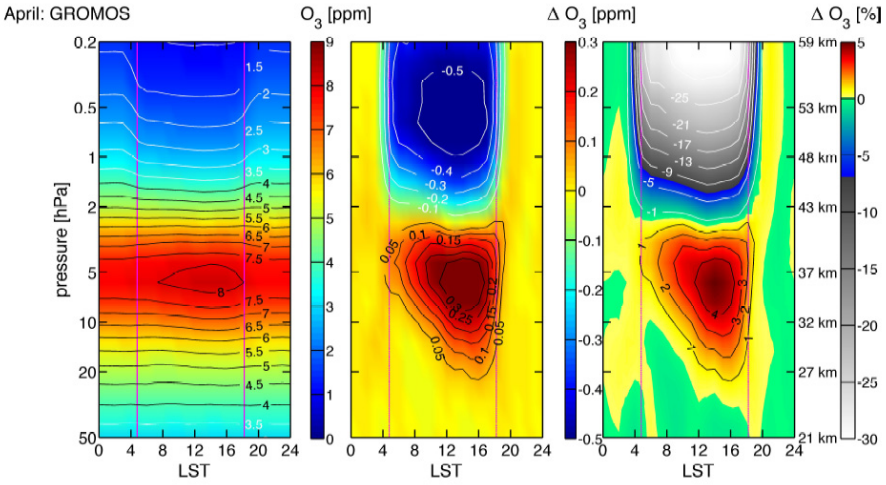

Fig. 3b. Same as Fig. 3a, but for the month of April.

ACPD
13, 22445–22485, 2013

Diurnal ozone variations above Bern

S. Studer et al.

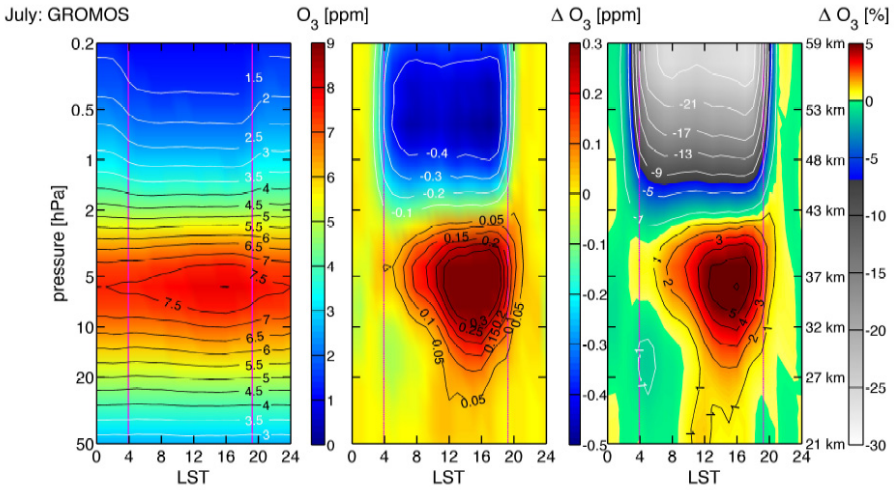

Fig. 3c. Same as Fig. 3a, but for the month of July.

ACPD
13, 22445–22485, 2013

Diurnal ozone variations above Bern

S. Studer et al.

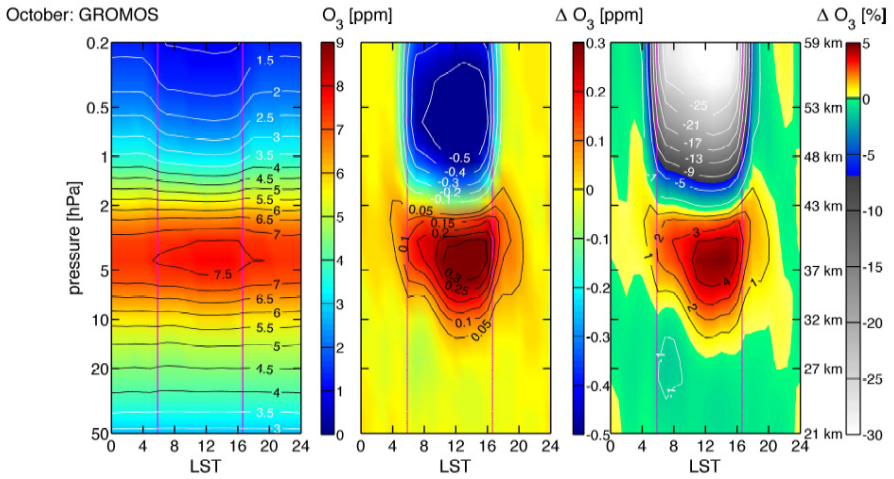

Fig. 3d. Same as Fig. 3a, but for the month of October.

ACPD
13, 22445–22485, 2013

Diurnal ozone variations above Bern

S. Studer et al.

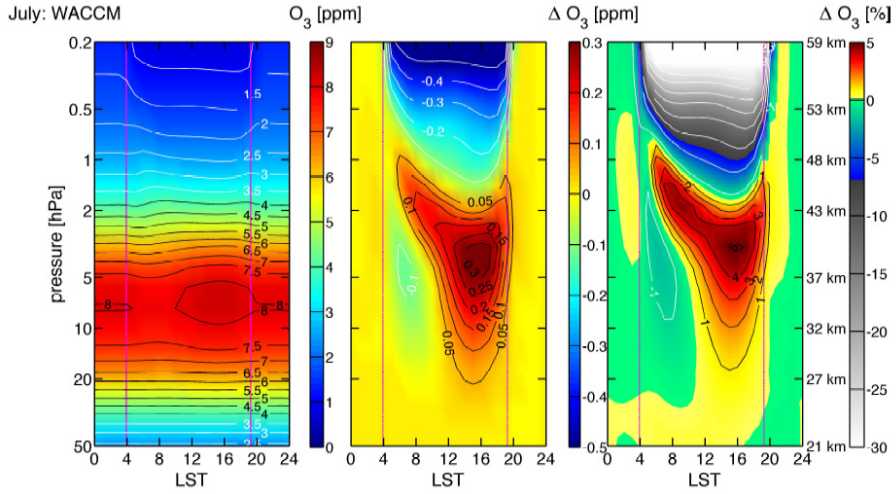

Fig. 4a. Mean diurnal ozone variation of WACCM between 50 and 0.2 hPa for July. The left, middle and right panel are described in Fig. 3a.

ACPD
13, 22445–22485, 2013

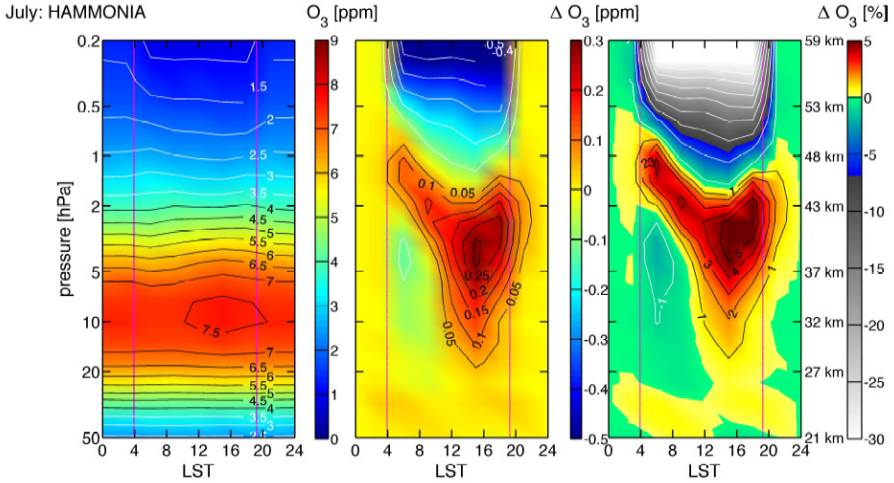

Fig. 4b. Mean diurnal ozone variation of HAMMONIA between 50 and 0.2 hPa for July. The left, middle and right panel are described in Fig. 3a.

ACPD
13, 22445–22485, 2013

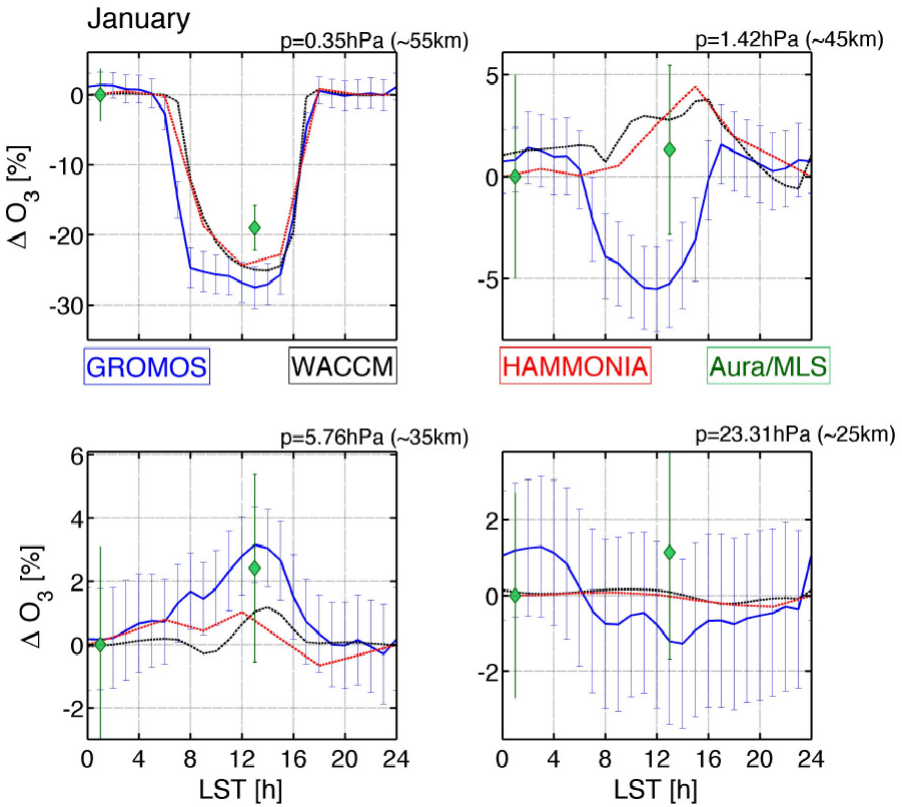

Fig. 5a. Relative mean differences for 4 different pressure levels in January. GROMOS is given by the blue line, while WACCM is given in black and HAMMONIA is given in red. The errorbars denote the mean standard deviation of GROMOS. Additionally, the relative mean difference between nighttime and daytime ozone of the two Aura/MLS overpasses is shown by the two green diamonds.

ACPD
13, 22445–22485, 2013

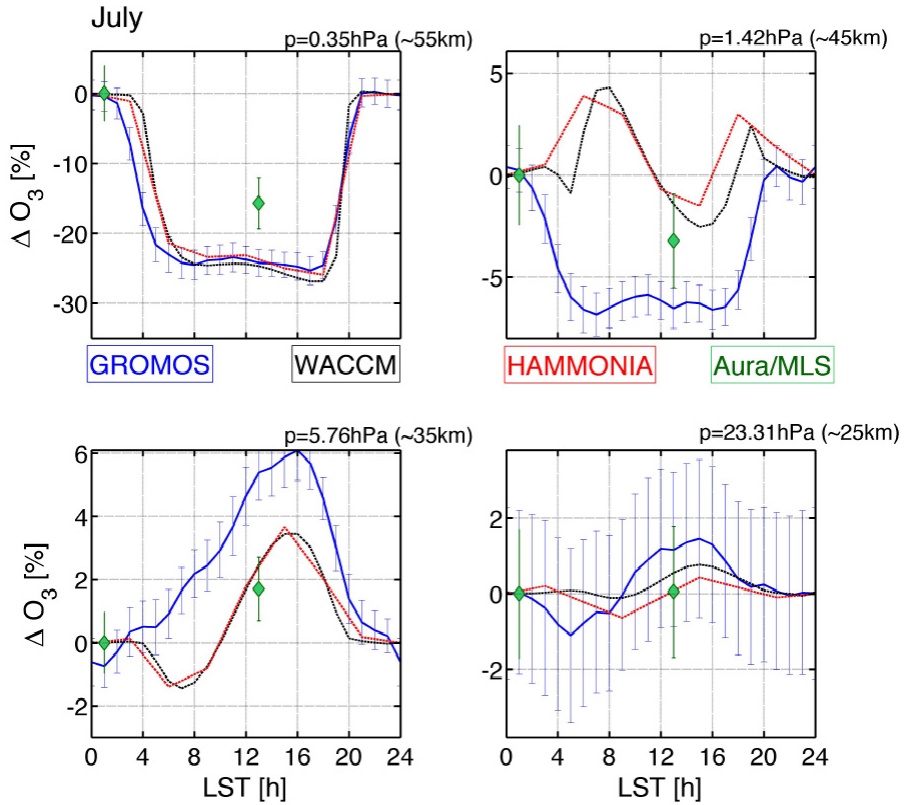

Fig. 5b. Same as Fig. 5a, but for the month of July.

ACPD
13, 22445–22485, 2013

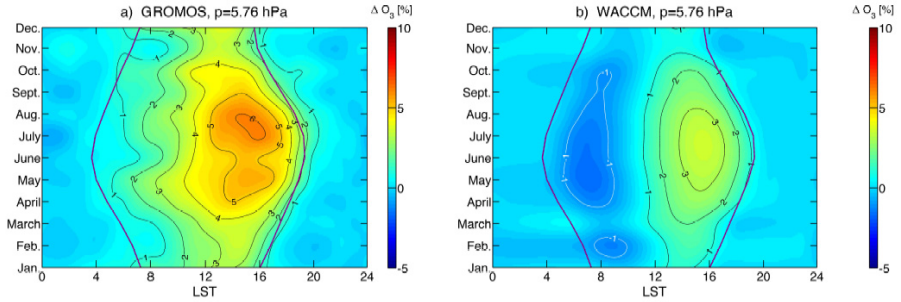

Fig. 6. Mean seasonal variation of diurnal ozone cycle of GROMOS **(a)** and WACCM **(b)** for a fixed pressure level in the stratosphere (5.76 hPa).

ACPD
13, 22445–22485, 2013

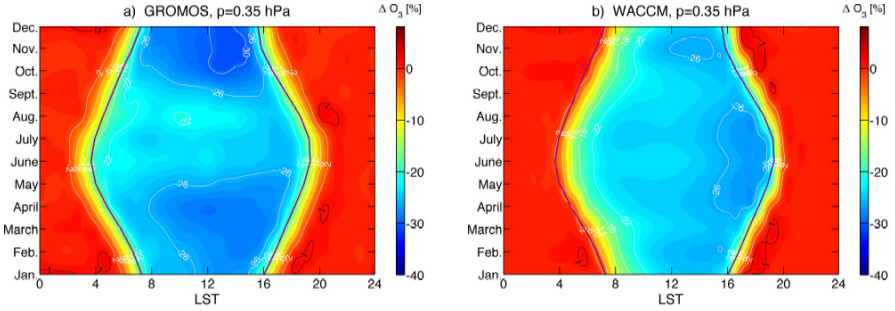

Fig. 7. Mean seasonal variation of diurnal ozone cycle of GROMOS **(a)** and WACCM **(b)** for a fixed pressure level in the mesosphere (0.35 hPa).

ACPD
13, 22445–22485, 2013

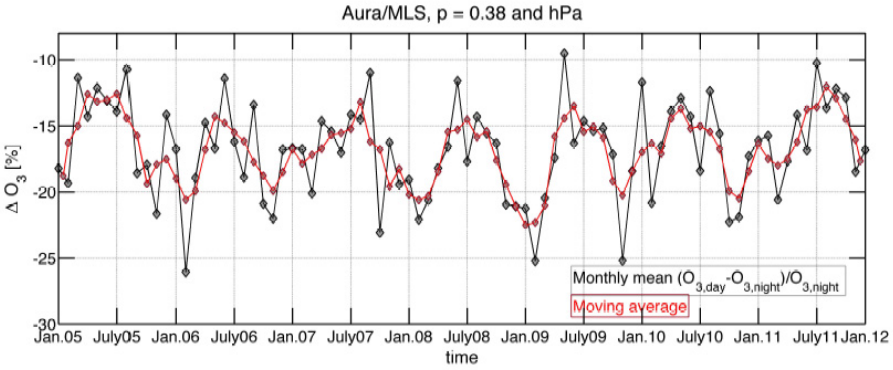

Fig. 8. Time series of relative mean difference between nighttime and daytime ozone values of Aura/MLS between January 2005 and December 2011. Grey diamonds show monthly mean values. A moving averaged of 3 month is applied (red).

ACPD
13, 22445–22485, 2013

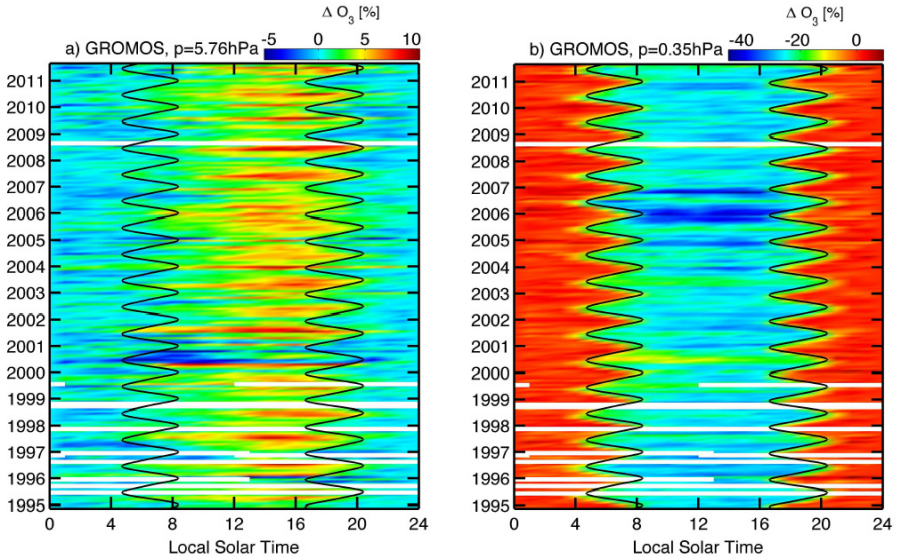

Fig. 9. Interannual variation of diurnal ozone cycle from 1995–2011. Pressure levels are the same as given in Fig. 6 and Fig. 7: **(a)** shows the interannual variation at 5.76 hPa, while **(b)** gives the interannual variation at 0.35 hPa.

ACPD
13, 22445–22485, 2013

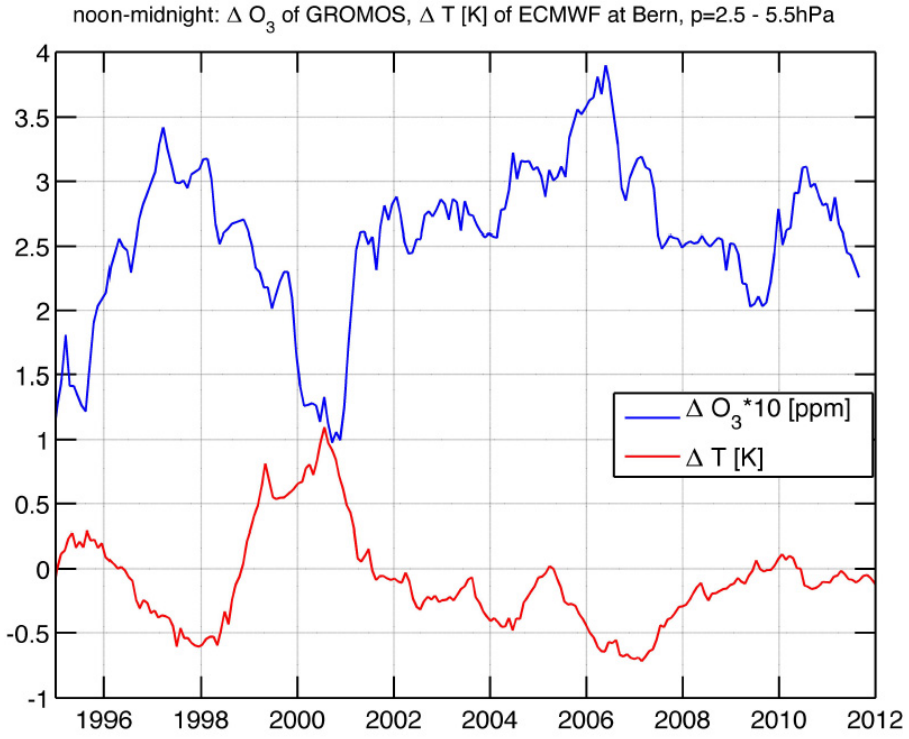

Fig. 10. Anticorrelation between day and night difference in temperature (ECMWF) and ozone (GROMOS) around 4 ± 1.5 hPa.

ACPD
13, 22445–22485, 2013